Available online at www.sciencedirect.com

ScienceDirect

Physics Procedia 83 (2016) 568 – 576

Physics Procedia

9th International Conference on Photonic Technologies - LANE 2016

Significance of the resonance condition for controlling the seam position in laser-assisted TIG welding

B. Emde[a,*], M. Huse[a], J. Hermsdorf[a], S. Kaierle[a], V. Wesling[a], L. Overmeyer[a], R. Kozakov[b], D. Uhrlandt[b]

[a]*Laser Zentrum Hannover e.V., Hollerithallee 8, 30419 Hannover, Germany*
[b]*Leibniz Institute for Plasma Science and Technology, Felix-Hausdorff-Str. 2, 17489 Greifswald, Germany*

Abstract

As an energy-preserving variant of laser hybrid welding, laser-assisted arc welding uses laser powers of less than 1 kW. Recent studies have shown that the electrical conductivity of a TIG welding arc changes within the arc in case of a resonant interaction between laser radiation and argon atoms. This paper presents investigations on how to control the position of the arc root on the workpiece by means of the resonant interaction. Furthermore, the influence on the welding result is demonstrated. The welding tests were carried out on a cooled copper plate and steel samples with resonant and non-resonant laser radiation. Moreover, an analysis of the weld seam is presented.

Peer-review under responsibility of the Bayerisches Laserzentrum GmbH

Keywords: TIG arc; resonant absorption; laser radiation

1. Introduction

The combination of a laser beam with an electrical arc in the laser hybrid welding process and its advantages have already been known for many years (Steen1979, Steen1980). In laser hybrid welding, typically several kW laser power is used. In contrast, laser-assisted arc welding uses laser powers below 1 kW, which allows the investment costs for the laser source to be reduced. Laser-assisted arc welding has been analyzed in a number of studies dealing with laser-assisted TIG welding (Cui1991, Cui1992, Hu2005a, Hu2005b, Hao2008, Barroi2012), laser-assisted

* Corresponding author. Tel.: +49-511-2788-336 ; fax: +49-511-2788-100 .
E-mail address: b.emde@lzh.de

Peer-review under responsibility of the Bayerisches Laserzentrum GmbH
doi:10.1016/j.phpro.2016.08.059

GMA welding (Stute2007, Liu2008, Hermsdorf2009a, Hermsdorf2013) and laser-assisted plasma welding (Fuerschbach1999, Mahrle2011, Mahrle2013, Schnick2012), using CO2 lasers, Nd:YAG lasers, fibre lasers or diode lasers.

In contrast to high laser power hybrid welding, laser-assisted arc welding does not allow deep welding, whereas the advantages of the process combination, like the increased welding speed or welding quality, are still present (Hermsdorf2009a). It is possible to quadruple the welding speed when combining arc and laser beam in one process zone (Cui1992). The additional energy of the laser radiation leads to an increase of metal vapour in the electrical arc and therewith raises the amount of the metal ions (Hu2002) which also leads to a change in the arc voltage and current (Steen1980). It is still unclear, if this change in the electrical arc's conductivity is responsible for the observed stabilization effect which allows an increase of the welding speed. Furthermore, an arc root fixed to the laser spot on the workpiece is observed. It allows the arc position to be controlled by pointing the laser beam to the target position on the workpiece (Schnick2012, Hermsdorf2009b), which is a huge advantage in industrial applications. For example, when welding butt joints in case of metal sheets of unequal thickness, it is possible to fix the arc on the deepest sheet in order to improve the seam quality (Hermsdorf2009a).

Further investigations have shown that an additional process optimization in terms of welding speed can be achieved, if the spectrum of the laser beam overlaps the emission lines of the used shielding gas (Hermsdorf2009a). Argon, a commonly used shielding gas, has many spectral lines between 700 and 1000 nm. Two transitions at 810 nm and 811 nm (Nist2016) are good candidates for interaction with laser, as they have high transition probabilities. With 811 nm centre wavelength and 2.5 nm line width, the used diode laser overlaps these argon emission lines (Hermsdorf2009a). Hermsdorf et. al. supposed that the resonant absorption of laser radiation leads to a change of the electrical conductivity of the arc which could be responsible for the stabilization of the arc (Hermsdorf2009a). This effect has already been known from optogalvanic spectroscopy where a laser beam propagates through a gas discharge and drives transitions between two electronic states of atoms or ions, causing a change of the population densities (Demtröder2003). The change of the population densities affects the discharge current because of a change of the ionization probabilities (Demtröder2003). A change of the optogalvanic current in an argon-filled glow discharge tube was demonstrated in (Matsuta2010). According to recent studies, the resonant absorption of laser radiation in a TIG welding arc changes the electrical conductivity of the arc (Emde2014, Emde2015, Kozakov2015a, Kozakov2015b). The resonant interaction between laser radiation and excited argon atoms depends on the welding current, the spatial overlap between laser beam and arc, the laser power and the centre wavelength (Emde2014, Emde2015). Based on these studies, a significant influence of the laser beam on the arc root and the possibility to control the arc root position with the laser beam position are expected. These effects are assumed to be more pronounced in case of resonant laser radiation. However, a systematic study of these suppositions has been missing so far.

The motivation for this investigation was to analyze the different laser beam influence on a TIG arc in case of resonant and non-resonant laser radiation. In addition, it is studied, if the resonant interaction between laser radiation and electrical arc can be exploited to improve the controlling of the arc root on the workpiece. The effect could be executed to compensate disturbances, like deformations, by moving the laser beam with a laser scanner system.

2. Experimental setup

The experimental setup is shown in Fig. 1. For the experiments, a standard current-controlled TIG welding source (MerkleLogiTIG 300 AC/DC) was used. To improve the accessibility of the arc root for the laser beam, the TIG torch was slanted 20° towards the welding direction 8 mm above the workpiece. Table 1 gives an overview of the welding parameters. The welding experiments were carried out on a cooled copper plate and 3 mm steel sheets (1.0330).

A 230 W laser beam (Laserline LDM 400-500) was focused on the workpiece with an angle of 30° in welding direction. At the beginning of each test, the focus of the laser beam was positioned directly under the electrode. The scanner allows movements of the laser focus across the welding direction. See Table 1 for further laser parameters. To test the influence of the resonant interaction, the centre wavelength of the laser beam was adjusted to the argon resonance wavelength of 811.3 nm and off resonance to 807.7 nm (see Fig. 2) for the same laser power.

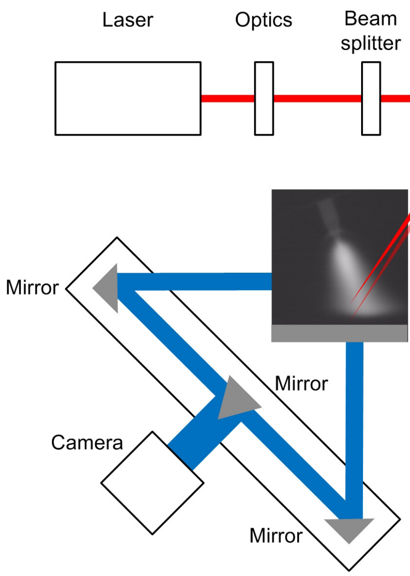

Fig. 1. Experimental setup.

To observe the electrical arc, a binocular vision system was used to synchronously take pictures of the arc from two different directions with one camera. Depending on the experiment, a compact camera (DCC 1545M) and a high-speed camera (MotionPro Y7 S3) were integrated in the experimental setup. The high-speed camera additionally provides a synchronized recording of the scanner position. To avoid the saturation by the laser radiation, a shortpass filter (cut-off wavelength: 700 nm) was integrated in front of the cameras.

Table 1. Welding and laser parameters.

Welding source	
Current	120 A DC
Gas	Ar 4.6
Gas flow	10 l/min
Welding speed for steel	240 mm/min
Stick-out	5 mm
Laser source	
Output power	230 W
Line width (FWHM) @ 230 W	2.5 nm
Focusing lens	300 mm
Collimation lens	50 mm
Fibre diameter	0.4 mm
Focus diameter	2.4 mm

As an example, Fig. 3 shows an image recorded with the binocular vision system. While on the left side the arc is shown in forward direction, the right side presents a side view of the arc. For an automated analysis, the arc angle was calculated from the centre of mass of the gray value distributions along the lines I and II.

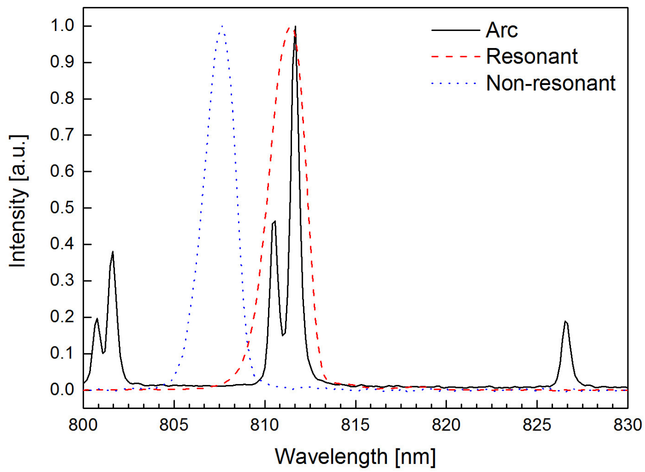

Fig. 2. Normalized arc emission spectrum and laser power spectra (resonant and non-resonant).

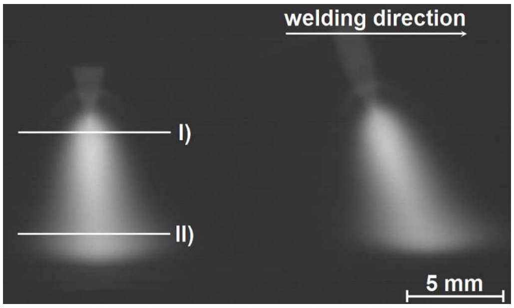

Fig. 3. Example for an arc image from two different directions.

3. Experimental Results

3.1. Reaction of the arc on a cooled copper plate

To demonstrate the influence of the resonant laser beam, experiments with the TIG arc burning on a cooled copper plate were carried out. Fig. 4 shows different binocular images of the arc when applying a laser beam at two different positions away from the arc root centre. In the images 4c and 4f, the difference of the above images visualizes the interaction zones of the laser radiation and the arc close to the focus position on the copper plate. For a better visualization, image 4c and 4f are inverted and intensified. The difference images show additional radiation in the overlap zone of the laser beam and the arc which is caused by the resonant interaction between laser radiation and excited argon atoms. Compared to Fig. 4, Fig. 5 shows the difference image of the arc in case of a deflected non-resonant laser beam. In this case, there is no additional radiation from the overlap zone.

For the characterization of the arc reaction, the arc angle was used. The laser spot on the plate was oscillated trapezoidally with a frequency of 0.4 Hz and a deflection of ±2.85 mm. The resulting arc angle curves are illustrated in Fig. 6. The curves represent the arc angle for each frame of a video sequence (9 frames per second). Only in the case of the resonant laser beam, the arc angle shows a cyclical change corresponding to the deflection of the laser beam, which can be explained by the resonant interaction between laser beam and excited argon atoms.

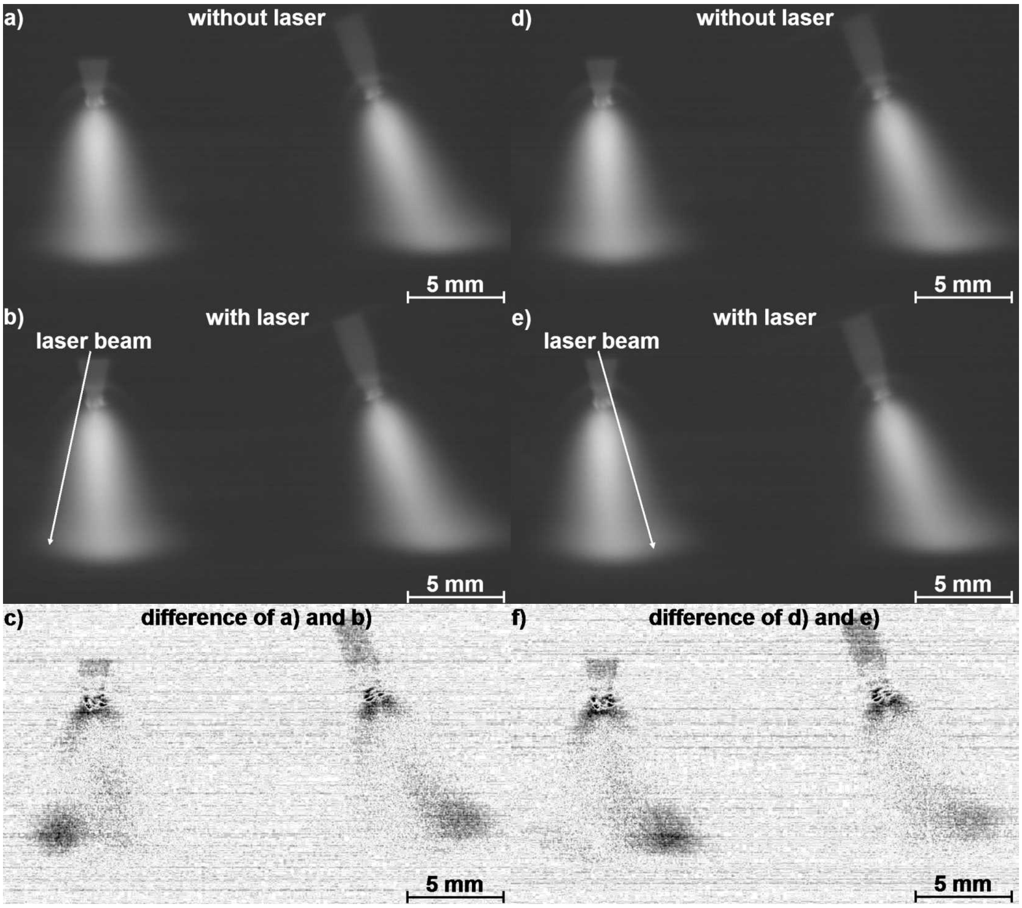

Fig. 4. Reaction of the arc in case of a deflected resonant laser beam (±2.85 mm) at positions on the left side of the arc root centre (a, b, and c) and on the right side (d, e, and f) (images were taken with the shortpass with a cut-off wavelength of 700 nm).

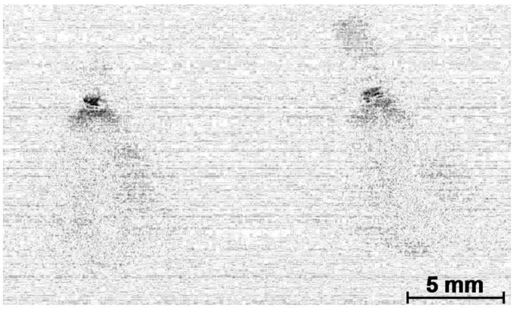

Fig. 5. Difference image in case of a deflected non-resonant laser beam (2.85 mm).

To control the arc root on the workpiece, knowledge about spatial limits and temporal performance of the laser beam impact on the arc angle is essential. Therefore, the reaction of the arc angle was analyzed with a laser beam which was oscillated trapezoidally with a deflection of ±7.60 mm for a TIG arc experiment on a cooled copper plate. Thereby, the laser beam 'moves' from -7.60 mm to 7.60 mm within 250 ms. For the maximum deflection of ±7.60 mm, no spatial overlap between laser beam and arc occurs. The sample rate of the used high-speed camera was set to 5000 frames per second. The determined arc angle for each frame of the video sequence and the laser beam deflection are illustrated in Fig. 7.

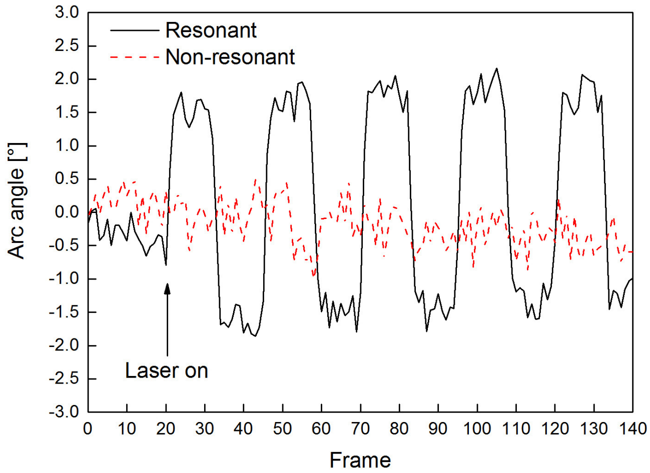

Fig. 6. Arc angle as function of the frame for an oscillated laser beam.

The arc angle curve can be divided in different sections attributed to the spatial overlap between laser beam and arc. Consequently, there is no change of the arc angle (zone 1) in case of no spatial overlap. In zone 2, the spatial overlap leads to an increase of the emitted radiation in the interaction zone. As a result, the arc angle 'moves' in the direction of the laser beam. In zone 3, the laser beam crosses the arc. Now the arc angle changes almost linearly with the laser beam's focus position. Afterwards, the spatial overlap between laser beam and arc starts to decrease which also decreases the arc angle (zone 4). Zone 5 is equivalent to zone 1, where the arc angle returns to the initial value. The temporal performance shows a good agreement with the given laser beam deflection in case of sufficient spatial overlap between laser beam and arc. Furthermore, Fig. 7 gives an answer about the maximum arc angle. The arc angle amplitude is approximately 3°.

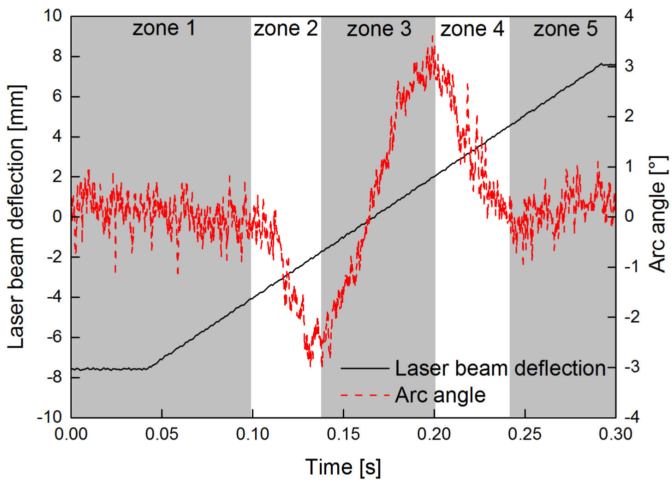

Fig. 7. Change of the arc angle, if the resonant laser beam crosses the arc.

3.2. Welding steel sheets with an oscillated laser beam

As shown in the previous chapters, a resonant laser beam can induce a change of the emitted radiation in the area of the interaction zone. Whether this change has a traceable influence on the welding joint was investigated by welding experiments on steel workpieces using resonant and non-resonant laser radiation. The laser beam was oscillated with a frequency of 0.3 Hz and a deflection of ±2.85 mm. The results are shown in Fig. 8. In both cases, an oscillated weld can be generated. Visually, there are no differences between resonant and non-resonant laser radiation. Furthermore, a change of the arc angle could be observed in experiment similar to 3.1 only in case of a resonant laser beam.

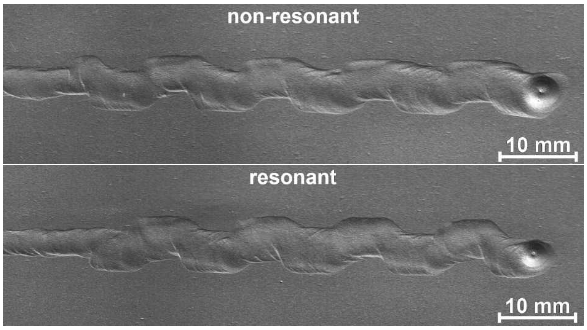

Fig. 8. Welding joints with oscillated resonant and non-resonant laser beam (welding direction from left to right; Material: 1.0330).

To gain information about the welding width, the surface profiles of the welds were measured using a perthometer. Based on these measurements, it is possible to determine the weld width. The weld width was measured six times in the area of the maximum laser beam deflection. In case of the resonant laser beam, the weld width was (6.70 ±0.18) mm, whereas in case of the non-resonant laser beam a weld width of (6.63 ±0.25) mm was achieved. Due to the measurement precision, it is not possible to detect an influence of resonant laser radiation on the welding joint.

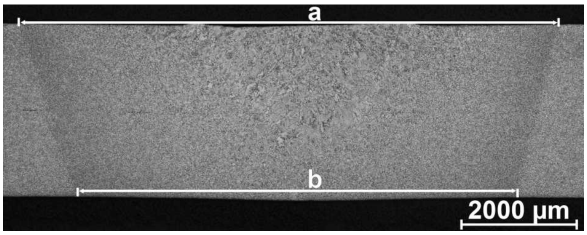

Fig. 9. Example of a cross-section.

Next to the weld width, the width of the heat-affected zone (HAZ) at the top side (a) and at the bottom side (b) of the workpiece were analyzed (see Fig. 9).The results are summarized in Table 2. No significant differences were found, indicating the minor relevance to meet the resonance condition for the whole area of the heat-affected zone. Consequently, the generation of an oscillated welding joint with the used setup is primarily attributed to additional heat input to the melt which is independent from the laser beam's wavelength.

Table 2. HAZ in case of deflected resonant and non-resonant laser beam.

	Non-resonant	Resonant
a in mm	9.73 ± 0.24	10.12 ± 0.23
b in mm	8.1 ± 1.1	9.07 ± 0.23

4. Conclusion

Resonant interaction between laser radiation and excited argon atoms in a TIG arc lead to an emission of additional radiation in their overlapping zone. As a measure of the elongation of the welding arc caused by a laser beam irradiation, the arc angle was defined. The arc angle is computed on the basis of the gray value distribution in images of the arc. In case of a resonant interaction of the laser beam with the welding arc, the arc angle correlates with the position of the laser spot because of additional light emitted from the interaction zone. For non-resonant laser radiation, no such additional light is emitted. Although the resonant interaction is supposed to increase the ionization probability in the interaction zone, neither the size of the heat-affected zone nor the seam width had a significant influence on meeting the resonance condition on the workpiece surface. In conclusion, since the position of the weld seam can reliably be controlled by the laser beam in either case, resonant as well as non-resonant, meeting the resonance condition in the laser-assisted TIG welding process does not dominate the welding result.

Acknowledgements

This work was supported by the German Research Foundation (DFG) under grant number WE 2846/11-1 and UH 106/7-1.

References

Barroi, A., Knill, R., Hermsdorf, J., Kaierle, S., Overmeyer, L., 2012. Laser Guided Double Tungsten Inert Gas Welding of Aluminium. In: Proceedings of 31st International Congress on Applications of Lasers & Electro-Optics (ICALEO), pp. 415-419.

Cui, H., 1991. Untersuchung der Wechselwirkungen zwischen Schweißlichtbogen und fokussiertem Laserstrahl und der Anwendungsmöglichkeiten kombinierter Laser-Lichtbogentechnik. Ph.D. thesis. TU Braunschweig.

Cui, H., Decker, I., Pursch, H., Ruge, J., Wendelsdorf, J., Wohlfahrt, H., 1992. Laserinduziertes Fokussieren des WIG-Lichtbogens. DVS-Berichte 146, 139-143.

Demtröder, W., 2003. Laser Spectroscopy: Basic Concepts and Instrumentation. Berlin: Springer-Verlag.

Emde, B., Huse, M., Hermsdorf, J., Kaierle, S., Wesling, V., Overmeyer, L., 2014. Influence of Welding Current and Focal Position on the Resonant Absorption of Laser Radiation in a TIG Welding Arc. In: Proceedings of 8thInternational Conference on Photonic Technologies LANE 2014, Physics Procedia 56, 646-652.

Emde, B., Huse, M., Hermsdorf, J., Kaierle, S., Wesling, V., Overmeyer, L., 2015. Influence of Laser Power and Wavelength on the Resonant Interaction between Laser Radiation and TIG Welding Arc. In Proceedings of Lasers in Manufacturing Conference 2015 (LIM2015).

Fuerschbach, P. W., 1999. Laser assisted plasma arc welding. In: Proceedings of International Congress on Applications of Lasers & Electro-Optics (ICALEO), San Diego, pp. 102-109.

Hermsdorf, J., Otte, F., Kling, R., 2009a. Development of the LGS-GMA welding process. In: Proceedings of the Fifth Internation WLT-Conference on Lasers in Manufacturing.

Hermsdorf, J., Beittoei, A., Fernandez, M. M., Pamin, S., Kling, R., 2009b. Development of a Laser Stabilized Gas Metal Arc Cladding Process. In: Proceedings of LAMP 2009 – the 5th International Congress on Laser Advanced Materials Processing.

Hermsdorf, J., 2013. Laserstabilisiertes Metallschutzgasschweißen mittels fasergeführten Festkörperlasern. Ph.D. thesis. Gottfried Wilhelm Leibniz Universität Hannover.

Hao, X., Song, G., 2008. Spectral analysis of the plasma in low-power laser/arc hybrid welding of magnesium alloy. IEEE Transactions on Plasma Science 36, 1-7.

Hu, B., 2002. Nd:YAG laser-assisted arc welding. Ph.D. thesis. Delft University of Technology.

Hu, B., Ouden, G., 2005a. Laser induced stabilisation of the welding arc. Science and Technology of Welding and Joining 10, 76-81.

Hu, B., Ouden, G., 2005b. Synergetic effects of hybrid laser/arc welding. Science and Technology of Welding and Joining 10, 427-431.

Kozakov, R., Emde, B., Pipa, A. V., Huse, M., Uhrlandt, D., Hermsdorf, J., Wesling, V., 2015a. Change of electrical conductivity of Ar welding arc under resonant absorption of laser radiation. Journal of Physics D: Applied Physics 48, 095502 (11pp.).

Kozakov, R., Gött, G.,Uhrlandt, D., Emde, B.,Hermsdorf, J.,Wesling, V., 2015b. Study of laser radiation absorption in a TIG welding arc. Welding in the World 59, 475-481.

Liu, L., Huang, R., Song, G., Hao, X., 2008. Behavior and spectrum analysis of welding ard in low-power YAG-laser-MAG hybrid-welding process. IEEE Transactions on Plasma Science 36, 1937-1943.

Mahrle, A., Schnick, M., Rose, S., Demuth, C., Beyer, E., Füssel, U., 2011. Process characteristics of fibre-laser-assisted plasma arc welding. Journal of Physics D: Applied Physics 44, 345502 (12pp.).

Mahrle, A., Rose, S., Schnick, M., Beyer, E., Füssel, U., 2013. Laser-assisted plasma arc welding of stainless steel lasergestütztes Schweißen. Journal of Laser Applications 25, 032006-1-032006-8.

Matsuta, H., Wagatsuma, K., Kitagawa, K., 2010. One and two-photon excited optogalvanic spectra of argon in the wavelength region of 735 - 850 nm. Analytical Science 26, 25–31.

NIST, 2014. Nist atomic spectra database. URL: http://physics.nist.gov/PhysRefData/ASD/lines form.html.
Schnick, M., Rose, S., Füssel, U., Mahrle, A., Demuth, C., Beyer, W., 2012. Experimental and numerical invstigation of the interaction between a plasma arc and a laser. Welding in the world 56, 93-100.
Steen, W.M., 1980. Arc augmented laser processing of materials. J. Appl. Phys. 51, 5636–5641.
Steen, W.M., Eboo, M., 1979. Arc-augmented laser welding. Metal Construction 7, 332–335.
Stute, U., Kling, R., Hermsdorf, J., 2007. Interaction between Electrical Arc and ND:YAG Laser Radiation, in: Annals of the CIRP.